BIOCHEMISTRY
including biophysical chemistry & molecular biology

ARTICLE

pubs.acs.org/biochemistry

Stabilization of the Second Oxyanion Intermediate by 1,4-Dihydroxy-2-naphthoyl-Coenzyme A Synthase of the Menaquinone Pathway: Spectroscopic Evidence of the Involvement of a Conserved Aspartic Acid

Minjiao Chen, Ming Jiang,[†] Yueru Sun, Zu-Feng Guo,[‡] and Zhihong Guo*

Department of Chemistry and State Key Laboratory for Molecular Neuroscience, The Hong Kong University of Science and Technology, Clear Water Bay, Kowloon, Hong Kong SAR, China

Supporting Information

ABSTRACT: 1,4-Dihydroxy-2-naphthoyl-coenzyme A (DHNA-CoA) synthase, or MenB, catalyzes an intramolecular Claisen condensation involving two oxyanion intermediates in the biosynthetic pathway of menaquinone, an essential respiration electron transporter in many microorganisms. Here we report the finding that the DHNA-CoA product and its analogues bind and inhibit the synthase from *Escherichia coli* with significant ultraviolet−visible spectral changes, which are similar to the changes induced by deprotonation of the free inhibitors in a basic solution. Dissection of the structure−affinity relationships of the inhibitors identifies the hydroxyl groups at positions 1 (C1-OH) and 4 (C4-OH) of DHNA-CoA or their equivalents as the dominant and minor sites, respectively, for the enzyme−ligand interaction that polarizes or deprotonates the bound ligands to cause the observed spectral changes. In the meantime, spectroscopic studies with active site mutants indicate that C4-OH of the enzyme-bound DHNA-CoA interacts with conserved polar residues Arg-91, Tyr-97, and Tyr-258 likely through a hydrogen bonding network that also includes Ser-161. In addition, site-directed mutation of the conserved Asp-163 to alanine causes a complete loss of the ligand binding ability of the protein, suggesting that the Asp-163 side chain is most likely hydrogen-bonded to C1-OH of DHNA-CoA to provide the dominant polarizing effect. Moreover, this mutation also completely eliminates the enzyme activity, strongly supporting the possibility that the Asp-163 side chain provides a strong stabilizing hydrogen bond to the tetrahedral oxyanion, which takes a position similar to that of C1-OH of the enzyme-bound DHNA-CoA and is the second high-energy intermediate in the intracellular Claisen condensation reaction. Interestingly, both Arg-91 and Tyr-97 are located in a disordered loop forming part of the active site of all available DHNA-CoA synthase structures. Their involvement in the interaction with the small molecule ligands suggests that the disordered loop is folded in interaction with the substrates or reaction intermediates, supporting an induced-fit catalytic mechanism for the enzyme.

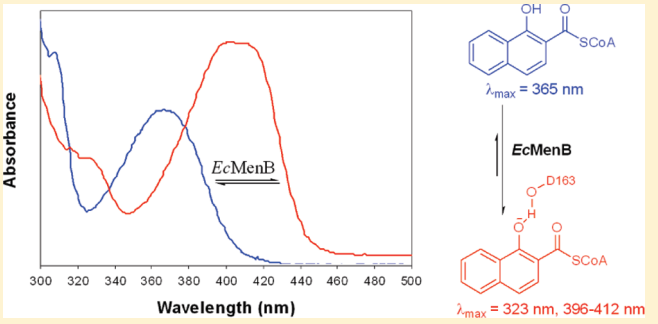

1,4-Dihydroxy-2-naphthoyl-CoA (DHNA-CoA) synthase, MenB (EC 4.1.3.36), converts *o*-succinylbenzoyl-CoA (OSB-CoA) to 1,4-dihydroxy-2-naphthoyl-CoA (DHNA-CoA) in the biosynthesis of menaquinone or vitamin K2, which is an obligate electron transport carrier in the respiratory chain of many microorganisms.[1] It catalyzes a multiple-step intramolecular Claisen condensation reaction involving an enolate intermediate to initiate the reaction, a tetrahedral oxyanion intermediate formed from the nucleophilic attack of the enolate on the electrophilic carboxyl group, and enolate intermediates in the late stage ketone−enol tautomerizations to form the naphthenoid ring of the product (Figure 1A). This is an irreversible multistep process pivotal in the biosynthesis of menaquinone that has been shown to be essential in a number of important microbial pathogens such as *Staphylococcus aureus*,[2] *Bacillus subtilis*,[3] and *Haemophilus influenzae*.[4] The DHNA-CoA synthase is thus an attractive target for development of antibacterial drugs, particularly in light of the proven lethality for the inhibition of menaquinone biosynthesis in microorganisms.[5,6]

Recent structural and biochemical studies have provided valuable insights into the catalytic mechanism of DHNA-CoA synthases. The first MenB crystallographic structure in complex with acetoacetyl-CoA shows that the protein adopts a typical crotonase family fold with an active site pocket consisting of amino acid residues highly conserved among proteins of different organisms.[7] As a conserved structural feature of all crotonase fold

Received: March 14, 2011
Revised: May 17, 2011
Published: May 31, 2011

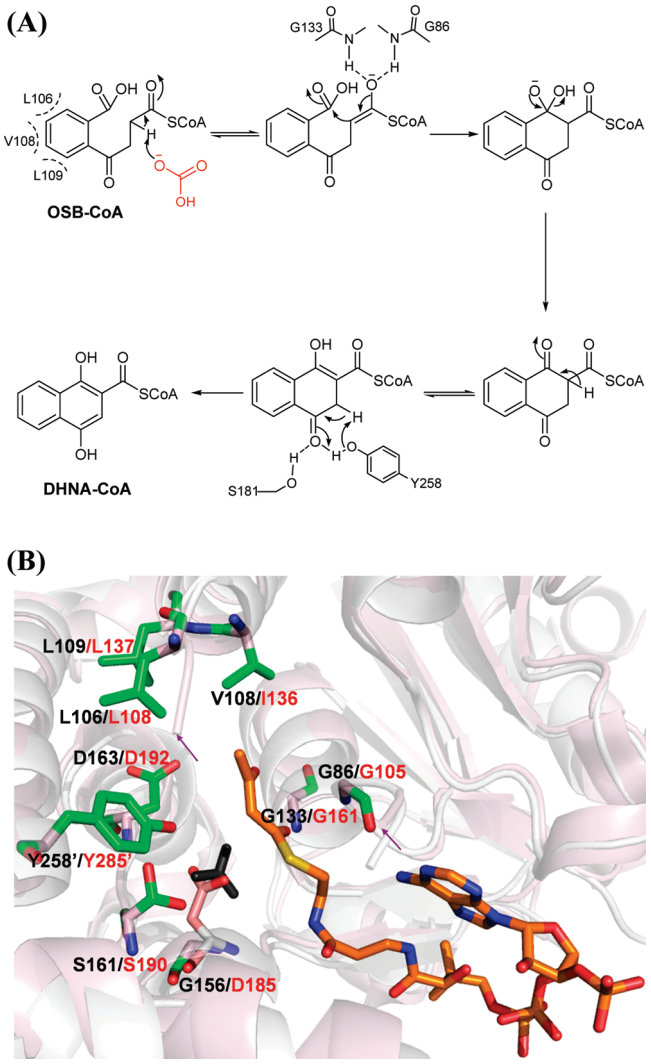

Figure 1. (A) Intramolecular Claisen condensation in the conversion of OSB-CoA to DHNA-CoA catalyzed by DHNA-CoA synthase of the menaquinone biosynthetic pathway. The reaction scheme is similar to that described in ref 19. The active site residues and the bicarbonate cofactor of *St*MenB or *Ec*MenB, which are essentially the same with 96.8% identical sequences, are shown only at selected reaction steps. (B) Conserved active site residues (sticks) of *St*MenB (salmon pink) superimposed with *Mtb*MenB (pale cyan) in complex with acetoacetyl-CoA (rainbow). The two structures (*St*MenB, PDB entry 3H02; *Mtb*MenB, PDB entry 1Q51) were superimposed with PyMol. The carbon atom of the bicarbonate cofactor is labeled in black, and the two arrows point to the two ends of a missing loop in *St*MenB with a KVRGDYGGYQDDSGV sequence (underlined residues highly conserved among the MenB proteins). D185 in *Mtb*MenB is represented as sticks with pink carbon atoms, whereas all other amino acid residues in stick presentation are from *St*MenB, which are labeled in black with their corresponding residues in *Mtb*MenB labeled in red. The primed residues in panel B are from a different subunit.

proteins,[8,9] the oxyanion hole is readily identified in the active site of this *Mycobacterium tuberculosis* protein (*Mtb*MenB) as consisting of the backbone amides of two conserved glycine residues for the stabilization of the thioester enolate intermediate to initiate the Claisen condensation. In addition, three conserved nonpolar residues in the proximity of the oxyanion hole form a hydrophobic patch for recognition and binding of the aromatic ring of the OSB-CoA substrate. Moreover, the polar groups of a conserved tyrosine and a conserved serine likely serve as hydrogen bond donors in substrate recognition and as general acids in the late-stage ketone−enol tautomerizations of the catalysis, while a conserved aspartate (Asp-192 in *Mtb*MenB) is believed to recognize and position the carboxyl group of the OSB-CoA substrate in catalysis. Identification of these active site residues and assignment of their catalytic roles have been strongly supported by site-directed mutagenesis at these positions, which eliminates or dramatically decreases the DHNA-CoA synthase activity.[7] These structural features and the active site pocket of *Mtb*MenB have been confirmed by independent crystallization and structural determination of the same protein.[10] In the meantime, similar active site pockets can be recognized and identified in the three-dimensional structures of MenB proteins from other species, including *S. aureus* (*Sa*MenB),[11] *Salmonella typhimurium* (*St*MenB, PDB entry 3H02), and *Geobacillus kaustophilus* HTA 426 (*Gk*MenB, PDB entry 2IEX).

Although there is abundant structural information about the MenB proteins, it is not straightforward to identify the catalytic base responsible for abstraction of a proton from the succinyl α-carbon of the OSB-CoA substrate. From the structure of *Mtb*MenB in complex with acetoacetyl-CoA,[7] a catalytically essential aspartate (Asp-185) occupies a position similar to that of the highly conserved acidic residue responsible for α-proton abstraction in reactions catalyzed by enoyl-CoA hydratases (crotonase) and enoyl-CoA isomerases[12−18] and is the most appropriate candidate for conducting the critical deprotonation reaction to initiate the intramolecular Claisen condensation. However, this likely catalytic role is at odds with the fact that this acidic residue is not conserved in multiple-sequence alignment, and a glycine occupies this position in many MenB proteins.[9] This dilemma has been resolved by the finding that an exogenous bicarbonate takes a position similar to that of the *Mtb*MenB Asp-185 side chain carboxylate and plays an essential catalytic role equivalent to that of the basic group in a large number of MenB proteins, such as *St*MenB and the orthologue from *Escherichia coli* (*Ec*MenB).[19] This finding suggests the presence of a conserved acidic group corresponding to *Mtb*MenB Asp-185 in all MenB proteins for α-proton abstraction in a unified catalytic mechanism. As a result of this finding, the MenB proteins are classified into two evolutionarily conserved subfamilies: the type I enzymes that contain a strictly conserved glycine at the position of *Mtb*MenB Asp-185 and use an exogenous bicarbonate as a cofactor in catalysis and the type II enzymes that are bicarbonate-independent and contain a strictly conserved aspartate at the critical position.

Despite the mechanistic insights illuminated by the structural and biochemical studies, it is still not clear how the tetrahedral oxyanion intermediate is stabilized in the MenB-catalyzed Claisen condensation. Similar tetrahedral oxyanion intermediates are widely involved in reactions catalyzed by proteases and α/β-hydrolases and are all stabilized by a structurally conserved oxyanion hole in these enzymes.[20,21] In the intermolecular Claisen condensation reactions catalyzed by the β-ketoacyl synthases in fatty acid or polyketide synthesis, the tetrahedral oxyanion intermediates are also found to be stabilized by a conserved oxyanion hole.[22−25] However, no apparent structural elements similar to these known oxyanion-stabilizing motifs can be assigned in the available MenB crystallographic structures for stabilization of the high-energy tetrahedral oxyanion intermediate. The identified oxyanion hole consisting of the backbone amides of two strictly conserved glycine residues in the MenB proteins is similar to

those found in all other members of the crotonase fold superfamily and is suitably located to stabilize the thioester enolate intermediate,[8,9] but not the spatially distant tetrahedral oxyanion intermediate resulting from the nucleophilic reaction of the enolate species.

In this report, we study the interaction of the type I MenB from *E. coli* with the DHNA-CoA product and its analogues in an attempt to shed light on the protein elements responsible for stabilization of the tetrahedral oxyanion intermediate in the catalytic mechanism. We found that the DHNA-CoA product and its analogues tightly bind the enzyme with significant changes in ultraviolet spectroscopic absorptions, which are indicative of ionization or polarization of the phenolic hydroxyl groups in the small molecule ligands by hydrogen bonding. Site-directed mutagenesis was subsequently used to identify the active site residues forming hydrogen bonds with the DHNA-CoA C1 hydroxyl group, which occupies a position similar to that of the oxyanion of the tetrahedral intermediate formed in the enzymatic intracellular Claisen condensation reaction. Through these investigations, we provide evidence of the involvement of a conserved aspartic acid in stabilization of the second oxyanion intermediate.

MATERIALS AND METHODS

Chemicals. The following chemical reagents were purchased from Sigma: $NaHCO_3$, salicylic acid, 3-hydroxybenzoic acid, 4-hydroxybenzoic acid, 2,3-dihydroxybenzoic acid, 2,4-dihydroxybenzoic acid, 3,4-dihydroxybenzoic acid, 3,5-dihydroxybenzoic acid, 1-hydroxyl-2-naphthoic acid, 2,4-dihydroxynaphthoic acid (DHNA), *N*-hydroxysuccinimide (NHS), *N*,*N*′-dicyclohexylcarbodiimide (DCC), α-ketoglutarate, thiamine diphosphate, coenzyme A, adenosine 5′-triphosphate, isopropyl β-D-thiogalactopyranoside (IPTG), buffers, and other salts.

Expression and Purification of Enzymes and Mutants. The proteins *Ec*MenB, *Bs*MenB, *Sa*MenB, *Ms*MenB, and *Mtb*MenB were obtained as previously described.[19] Reported procedures were followed to express and purify the following enzymes to homogeneity as hexahistidine-tagged proteins: EntC,[26,27] MenD,[28,29] MenC,[28] MenH,[30,31] and MenE.[30] The site-directed *Ec*MenB mutations were created with the QuikChange site-directed mutagenesis kit (Stratagene) using the plasmid for expression of the wild-type *Ec*MenB without any tag as a template. The following oligodeoxynucleotide primers were used in the mutagenic reactions: CGG CGG CTT TAA AGA TGA TTC C and GGA ATC ATC TTT AAA GCC GCCG for Y97F, GCG TGG TGA TTT CGG CGG CTA TAA AG and CTT TAT AGC CGC CGA AAT CAC CAC GC for Y94F, GGT GAC CAG AAA GTG GCT GGT GAT TAC GGC GG and CCG CCG TAA TCA CCA GCC ACT TTC TGG TCA CC for R91A, CAT GCT GTT CTT CAT GAC GGA AGA AGG TC and GAC CTT CTT CCG TCA TGA AGA ACA GCA TG for Y258F, GGT TCC TTC GAG GGC GGC TGG GGC G and CGC CCC AGC CGC CCT CGA AGG AAC C for D163E, GGT TCC TTC AAC GGC GGC TGG GGC G and CGC CCC AGC CGC CGT TGA AGG AAC C for D163N, and GAA AGT CGG TGC CTT CGA CGG CG and CGC CGT CGA AGG CAC CGA CTT TC for S161A. The cloned inserts of all the mutant plasmids were verified to contain only the intended mutation by full-length DNA sequencing. As in the purification of wild-type *Ec*MenB,[19] the site-directed mutants were purified using a combination of ammonium sulfate fractionation, DEAE chromatography, and size-exclusion chromatography using Sephacryl S-200 beads (GE Healthcare).

Synthesis of SHCHC and Thioesters. Chorismate was isolated from an engineered bacterial strain[32] and used as the starting material in chemoenzymatic synthesis of (1*R*,6*R*)-2-succinyl-6-hydroxy-2,4-cyclohexadiene-1-carboxylate (SHCHC) using EntC, MenD, and MenH as previously described.[30] 1-Hydroxy-2-naphthoyl-CoA (1-HNA-CoA) was synthesized from 1-hydroxynaphthoic acid using a two-step procedure,[33] whereas all other CoA thioesters were obtained via the same synthetic method from previous studies.[30,34] It was obtained in 28.7% yield after HPLC purification with a reported method.[34] 1-Hydroxynaphthoyl-CoA: ^{1}H NMR (methanol-d_4, 400 MHz) δ 8.76 (s, 1H, adenine H), 8.33 (d, J = 8.1 Hz, 1H, adenine H), 8.16 (s, 1H), 7.85 (m, 2H), 7.71 (m, 1H), 7.56 (m, 1H), 7.45 (m, 1H), 6.44 (d, J = 6.0 Hz, 1H, ribose anomeric H), 4.98 (m, 1H), 4.67 (s, 2H), 4.40 (s, 1H, ribose H), 4.22 (s, 1H, ribose CHO), 4.19 (s, 1H), 3.72 (m, 1H), 3. 59 (m, 2H), 3.61 (m, 2H), 3,55 (m, 2H), 2.50 (t, J = 6.6 Hz, 2H), 1.14 (s, 3H, Me), 0.83 (s, 3H, Me).

Enzyme Activity Assays. A 50 mM sodium phosphate buffer (pH 7.0) was used for the activity assay of *Ec*MenB and its mutants using a reported method[19] when sodium bicarbonate was not added. To prevent a change in pH, 200 mM sodium phosphate (pH 7.0) was used for the assay when 10−20 mM $NaHCO_3$ was included in the reaction mixture. Briefly, the MenB substrate OSB-CoA was prepared in situ via addition of MenC and MenE to a reaction mixture containing 1−30 μM SHCHC, 200 μM ATP, 200 μM CoA-SH, 1 mM DTT, and 10 mM $MgCl_2$ for incubation at room temperature for 15 min. Subsequently, *Ec*MenB or its mutant was added to the mixture for monitoring of the formation of DHNA-CoA at 392 nm. In the inhibition studies, the enzyme was preincubated with the thioester inhibitor at a varied concentration for 8 min before addition to the reaction mixture to determine the initial reaction rate. A Nova-Pak C18 column (4 μm particle size, 3.9 mm × 150 mm) was used for HPLC analysis of the reaction products, if necessary, using isocratic elution with 1% formic acid in water at a rate of 1 mL/min.

Enzyme−Ligand Interaction. The UV−vis spectrum of a mixture of the bound small molecule ligand and *Ec*MenB or its mutants was recorded in 50 mM sodium phosphate (pH 7.0) in the absence of sodium bicarbonate or in 200 mM sodium phosphate (pH 7.0) in the presence of 10−20 mM sodium bicarbonate. The absorptions of the protein at the same concentration were subtracted from that of the mixture to obtain the spectrum of the small molecule ligand. To study the spectroscopic changes of the small molecule ligands upon deprotonation, the UV−vis spectra of the CoA thioesters were determined at a fixed concentration in 50 mM sodium phosphate with a pH value varied from 5.5 to 14.

Isothermal titration calorimetry (ITC) was used to determine the binding affinity (K_a), enthalpy change (ΔH), and binding stoichiometry (n) of the interaction between the thioesters and *Ec*MenB or its mutants. The measurements were performed on a Microcal VP-ITC calorimeter at 25 °C. All protein samples (at ∼0.012 mM) were in 200 mM phosphate buffer (pH 7.0) containing 20 mM $NaHCO_3$. The titration was conducted via injection of 5−10 μL aliquots of the thioesters (at a concentration 4−6-fold higher than that of the protein) at time intervals of 6 min to ensure that the titration peak returned to the baseline. The titration data were analyzed with Origin 7.0 and curve-fitted by the one-site binding model.

Structure Analysis and Modeling. All structures were generated using PyMol 1.0[35] from *Sa. typhimurium* MenB (PDB entry 3H02) and *M. tuberculosis* MenB (PDB entry 1Q51) using SWISS-MODEL. DHNA-CoA was modeled into the *St*MenB active site using Coot.[36]

RESULTS AND DISCUSSION

Tight Binding Interaction between DHNA-CoA and *Ec*MenB. Before *Ec*MenB was known to strictly depend on exogenous bicarbonate for its DHNA-CoA synthase activity,[19] the enzyme was assayed in the absence of added bicarbonate and consequently exhibited only a low level of activity that was due to the small amount of bicarbonate resulting from solvation of air carbon dioxide in buffer. As a result, a large amount of the enzyme had to be included in the assays to observe its DHNA-CoA synthase activity with ease. We noticed an unusual absorption peak in the ultraviolet−visible (UV) spectrum of the reaction product from such enzyme assays. In addition to the absorption peak at 396 nm that was consistent with the characteristic DHNA-CoA absorption at 392 nm, there was an additional absorption peak at 348 nm, which coincided with the typical UV absorption peak of DHNA, the hydrolytic product of DHNA-CoA, at 352 nm (Figure 2A). We suspected that *Ec*MenB was also responsible for the conversion of DHNA-CoA to DHNA to give rise to the extra absorption peak at 348 nm, in light of the fact that the DHNA-CoA hydrolysis was a step not included in the *E. coli* menaquinone biosynthesis.[19] However, HPLC analysis failed to detect DHNA in the reaction products (data not shown).

The unusual absorption peak did not turn out to be from a new product in the reaction. The UV−vis spectrum of the reaction product was successfully reproduced by incubating excess *Ec*MenB with synthetic DHNA-CoA; the 392 nm absorption of free DHNA-CoA was shifted to 396 nm, and a new absorption peak at 348 nm was formed (Figure 2A). Interestingly, no free chromogenic species was detected in the ultrafiltration filtrate of the incubation mixture, suggesting that all DHNA-CoA was associated with the protein in a stable complex (see Figure S3A of the Supporting Information). To determine the nature of the tight association between *Ec*MenB and DHNA-CoA, 0.05% SDS was used to denature the protein in the complex. As a result, the UV absorption associated with formation of the complex at 348 nm disappeared and the UV absorption spectrum of the resulting solution changed drastically to be exactly identical to that of free DHNA-CoA (Figure S3B of the Supporting Information). In addition, similar results were obtained when the complex was denatured with 0.1 N HCl (Figure S3C of the Supporting Information). In both denaturing experiments, the resulting solution was found to contain DHNA-CoA only but no DHNA by HPLC analysis (data not shown). These results unambiguously demonstrate that that the tight binding interaction between *Ec*MenB and DHNA-CoA is reversible and noncovalent.

The observed spectroscopic changes of the bound DHNA-CoA were found to be sensitive to the ionic strength of the solution. When the buffer was changed from 50 mM sodium phosphate (pH 7.0) to 200 mM sodium phosphate (pH 7.0), the long-wavelength absorption of DHNA-CoA in the complex was red-shifted from 392 to 405 nm while the new absorption peak at 348 nm was essentially unchanged (Figure 2B). However, these spectral changes were not affected by inclusion of externally added bicarbonate up to 20 mM (data not shown), indicating

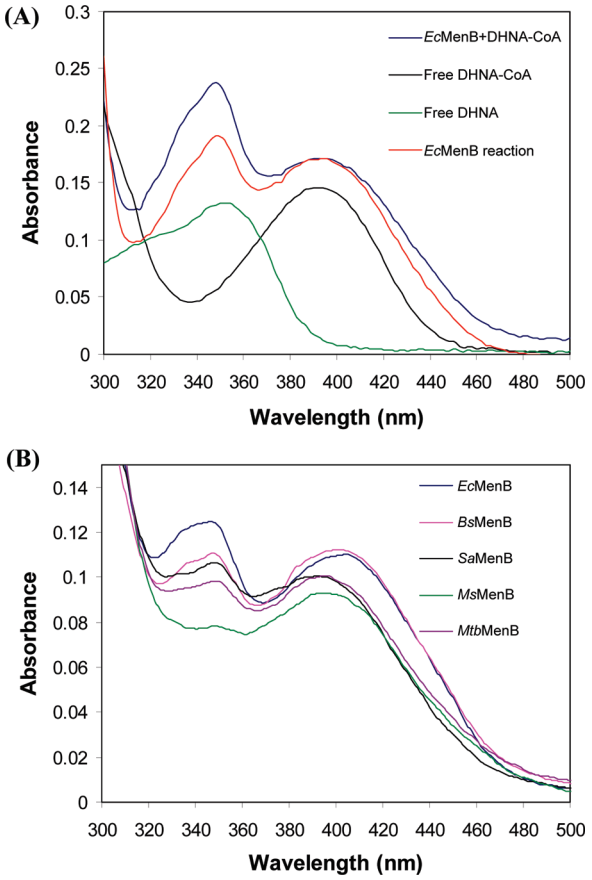

Figure 2. (A) New absorption peak at 348 nm from the interaction between *Ec*MenB and DHNA-CoA. *Ec*MenB+DHNA-CoA: incubation product of 37.6 μM *Ec*MenB and 18.5 μM DHNA-CoA in 50 mM phosphate buffer (pH 7.0). Free DHNA-CoA and DHNA were in 50 mM phosphate buffer (pH 7.0). *Ec*MenB reaction: product resulting from a 1 h reaction at room temperature in a mixture containing 618 μg/mL *Ec*MenB, 3.5 μg/mL MenE, 1.0 μM MenC, 25 μM SHCHC, 200 μM ATP, 200 μM CoA-SH, 0.5 mM DDT, and 10 mM $MgCl_2$ in 50 mM phosphate buffer (pH 7.0). (B) UV−vis spectra of DHNA-CoA after incubation with various MenB proteins. The concentration of DHNA-CoA was 12 μM, and the solution contained 200 mM sodium phosphate (pH 7.0) and 20 mM $NaHCO_3$. The concentrations of the proteins were as follows: 24 μM *Ec*MenB, 24 μM *Bs*MenB, 24 μM *Sa*MenB, 9.3 μM *Ms*MenB, and 17 μM *Mtb*MenB.

that binding of bicarbonate to the *Ec*MenB active site had little effect on the interaction of DHNA-CoA with the enzyme.

Interaction of DHNA-CoA with MenB Proteins from Other Bacteria. Two additional type I MenB proteins from *S. aureus* (*Sa*MenB) and *B. subtilis* (*Bs*MenB) and two type II MenB proteins from *M. tuberculosis* (*Mtb*MenB) and *Mycobacterium smegmatis* (*Ms*MenB) were tested in interaction with DHNA-CoA. A new absorption peak was observed at 348 nm for interaction of the small molecule with all the tested proteins in 200 mM sodium phosphate buffer (pH 7.0) (Figure 2B). In addition, similar to the effects of *Ec*MenB binding, the longest-wavelength absorption of DHNA-CoA is also red-shifted to varying extents. *Bs*MenB is the same as *Ec*MenB in causing a 14 nm red shift of the DHNA-CoA absorbance at 392 nm in the binding interaction, whereas *Sa*MenB, *Ms*MenB, and *Mtb*MenB cause a red shift of only <4 nm. Again, these spectral changes were not affected by inclusion of bicarbonate at a concentration

Table 1. Red Shifts of the Longest-Wavelength Absorption of DHNA-CoA Analogues in the Presence of *Ec*MenB and Parameters for the Binding Interaction

	no enzyme		saturating *Ec*MenB[a]				
analogue	λ_{max} (nm)	ε (mM^{-1} cm^{-1})	λ_{max} (nm)	ε (mM^{-1} cm^{-1})	n[b]	K_D (μM)[c]	K_I (μM)[d]
1-HNA-CoA	368	8.20	408	8.98	0.50 (0.51)	0.11 ± 0.03	1.3 ± 0.3
salicylyl-CoA	318	5.37	380	7.13	0.48 (0.37)	0.45 ± 0.07	6.0 ± 2.2
2,3-DHB-CoA	340	0.79	390	2.68	0.66 (0.64)	0.18 ± 0.03	3.1 ± 1.1
2,4-DHB-CoA	319	8.28	368	7.70	0.51 (0.54)	0.44 ± 0.06	2.2 ± 0.7
3,4-DHB-CoA	260	17.8	260	17.8	nd[e]	nd[e]	nd[e]
3,5-DHB-CoA	260	17.8	260	17.8	nd[e]	nd[e]	nd[e]
3-HB-CoA	262	21.3	262	21.3	nd[e]	nd[e]	nd[e]
4-HB-CoA	262	21.4	262	21.4	nd[e]	nd[e]	nd[e]

[a] The analogue is considered to be saturated by *Ec*MenB when the position of its longest-wavelength absorption (λ_{max}) and its intensity (represented by the extinction coefficient ε) no longer change with increasing enzyme concentration. [b] n is the number of the DHNA-CoA analogues bound by one subunit of *Ec*MenB. The value was obtained by spectroscopic titration [or by isothermal titration calorimetry (in parentheses)]. [c] The dissociation constant (K_D) was determined by isothermal titration calorimetry at 25 °C. [d] The inhibition constant (K_I) was determined at room temperature (23 °C). [e] Not detected.

up to 20 mM in the buffer. These similarities in the observed UV−vis spectral changes of DHNA-CoA show that the binding interaction with the thioester is not limited to *Ec*MenB, but a general feature of all DHNA-CoA synthases.

Characterization of DHNA-CoA Binding and Inhibition of *Ec*MenB. To determine the binding stoichiometry, a DHNA-CoA solution was titrated with *Ec*MenB. The amount of the stable complex indicated by the absorbance at 348 nm increased linearly with enzyme concentration and leveled off at an enzyme:ligand ratio of 1.75 (Figure S4A of the Supporting Information), corresponding to the binding of one small molecule ligand by every two *Ec*MenB subunits. Similar half-of-sites binding of small molecule ligands is often found for other oligomeric enzymes in solution or crystalline states.[37−39] Further quantification of the *Ec*MenB−DHNA-CoA interaction was next attempted with isothermal titration calorimetry (ITC). However, the titration result was complicated by the exothermic decomposition of DHNA-CoA during the titration process. Addition of thiol-protecting agents such as thionite or DDT (they caused additional interference with the ITC results) or saturation of the solutions with argon did not eliminate the adverse effects. After subtraction of the contribution of heat from spontaneous DHNA-CoA decomposition, the dissociation constant (K_d) of the complex of DHNA-CoA with *Ec*MenB was eventually estimated to be less than 500 nM, consistent with the observed formation of a stable complex between them.

The strong binding interaction between *Ec*MenB and DHNA-CoA suggests product inhibition of the enzyme. Indeed, the enzyme activity was found to be inhibited by synthetic DHNA-CoA in a concentration-dependent manner. The Lineweaver−Burk plots of the enzymatic reaction in the presence of the product at a varied concentration were found to have approximately the same intercept on the vertical axis (Figure S4B of the Supporting Information), suggesting competitive inhibition. The inhibition constant (K_I) was determined to be 1.5 ± 0.4 μM, significantly larger than the K_D of the ligand−enzyme complex. These kinetic results support the observation that DHNA-CoA competes with the enzyme substrate (OSB-CoA) and binds to the active site of *Ec*MenB. The difference between K_I and K_D of DHNA-CoA is probably due to the observed half-sites binding of the ligand to *Ec*MenB in the spectroscopic titration experiment.

Binding and Inhibition of *Ec*MenB by DHNA-CoA Analogues. To identify the DHNA-CoA structural components making direct contacts with *Ec*MenB, a number of DHNA-CoA analogues were synthesized and studied for their interaction with the enzyme. As in the case of the 14 nm red shift and intensification observed for long-wavelength absorption of DHNA-CoA in 200 mM sodium phosphate (pH 7.0), the following analogues were found to interact with *Ec*MenB with a 32−64 nm red shift and an increased intensity for the long-wavelength absorption peak (Table 1) in the same buffer: 1-hydroxy-2-naphthoyl-CoA (1-HNA-CoA), salicylyl-CoA (or 2-hydroxybenzoyl-CoA, 2-HB-CoA), 2,3-dihydroxybenzoyl-CoA (2,3-DHB-CoA), and 2,4-dihydroxybenzoyl-CoA (2,4-DHB-CoA). Besides the significant spectroscopic changes, these analogues were found to bind *Ec*MenB in a ratio of 0.37−0.66 small molecule ligand per protein monomer, similar to the ratio of 0.57 for the interaction of DHNA-CoA with *Ec*MenB. In addition, the binding DHNA-CoA analogues were also found to be competitive inhibitors of the enzyme with an inhibition constant (K_I) in the micromolar range and a submicromolar dissociation constant (K_D) (Table 1). All these results support the observation that the DHNA-CoA analogues bind to the *Ec*MenB active site in the same mode as DHNA-CoA. On the other hand, 3-hydroxybenzoyl-CoA (3-HB-CoA), 4-hydroxybenzoyl-CoA (4-HB-CoA), 3,4-dihydroxybenzoyl-CoA (3,4-DHB-CoA), and 3,5-dihydroxybenzoyl-CoA (3,5-DHB-CoA) were not found to interact with *Ec*MenB by either UV−vis spectroscopy or isothermal titration calorimetry (Table 1).

One important difference between the binding and nonbinding DHNA-CoA analogues is that the former contains a hydroxyl group in the same relative position with respect to the thioester function as the C1-OH of DHNA-CoA, whereas the latter does not have such a hydroxyl group. Noticeably, both 3-HB-CoA and 3,5-DHB-CoA contain a phenolic hydroxyl group in the same relative position with respect to the thioester function as the C4-OH of DHNA-CoA but are unable to bind the enzyme like salicylyl-CoA (or 2-HB-CoA). These differences strongly suggest that the high-affinity interaction between DHNA-CoA and *Ec*MenB is mainly due to the interaction of active site residues with both C1- and C4-hydroxyl groups of the small molecule ligand, of which the former makes a far greater contribution than

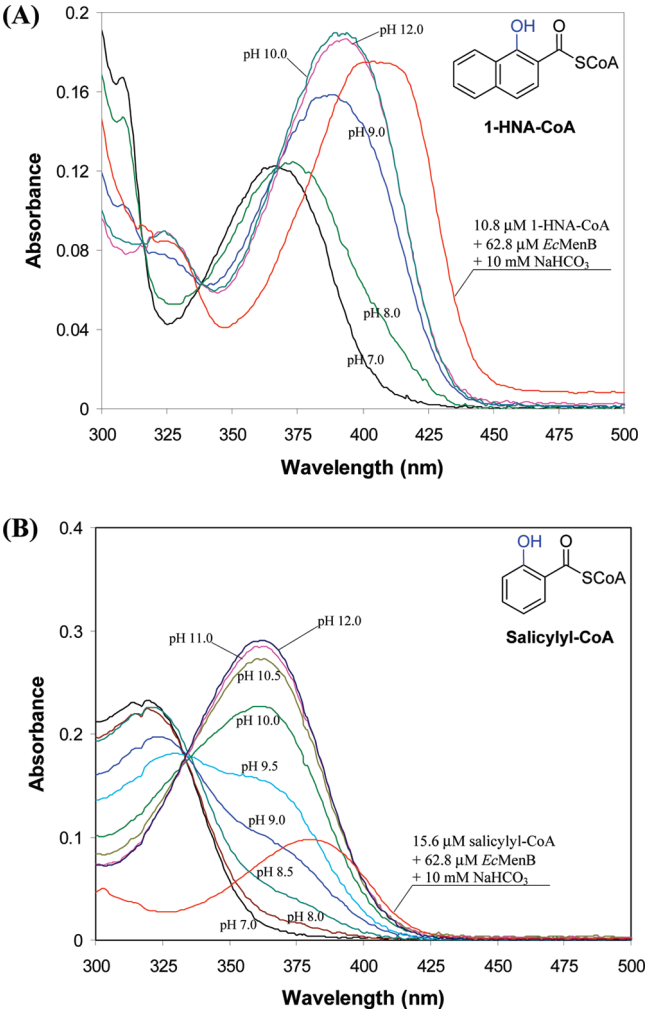

Figure 3. Red shifting of the long-wavelength absorption of 1-HNA-CoA (A) and salicylyl-CoA (B) in increasingly basic solutions. For comparison, the UV−vis spectra of the *Ec*MenB-bound ligands are presented in red [200 mM sodium phosphate and 10 mM $NaHCO_3$ (pH 7.0)]. The concentrations of 1-HNA-CoA and salicylyl-CoA in the pH titration were 40 and 60 μM, respectively.

the latter. This is supported by the similar submicromolar dissociation constants for 1-HNA-CoA and other binding analogues in comparison to DHNA-CoA (K_D < 500 nM). The 4-fold difference in K_D between 1-HNA-CoA and salicylyl-CoA (Table 1) suggests that the hydrophobic interaction between the enzyme active site and the unfunctionalized aromatic ring of either 1-HNA-CoA or DHNA-CoA contributes much less to the binding affinity than the C1-OH interaction.

Comparison of the spectral changes for 1-HNA-CoA and DHNA-CoA revealed that the interaction at C1-OH of DHNA-CoA with *Ec*MenB also likely plays a major role in the electronic structural change of the ligand, which is indicated by the observed changes in the electronic absorptions. Besides the similar red shifts and intensification for the long-wavelength absorption peak that may have split into two peaks to form a plateau (from 397 to 413 nm) centered at 408 nm, the enzyme-bound 1-HNA-CoA was also found to have an additional electronic peak at 325 nm (Figure 3A), which closely resembles the new 348 nm absorption for the enzyme-bound DHNA-CoA. The difference in the relative intensity of the new absorption and the red-shifted peak between 1-HNA-CoA (Figure 3A) and DHNA-CoA (Figure 2B) may be caused by additional interaction of C4-OH of DHNA-CoA with the *Ec*MenB active site residues, which is absent in the binding of 1-HNA-CoA. Taken together, the experimental results for the DHNA-CoA analogues strongly support the possibility that C1-OH of DHNA-CoA dominates the high-affinity interaction of the small molecule ligand with the enzyme to cause the observed spectral changes.

Phenolic Deprotonation and Enzyme Binding Cause Similar Spectral Changes in DHNA-CoA Analogues. The red shifts of the UV−vis spectra of the DHNA-CoA analogues are very similar to that observed for the Δ^5-3-ketosteroid isomerase (KSI)-bound enol, phenol, or naphthol inhibitors.[40] The cause of the spectral changes of the KSI inhibitors was once a topic of intense investigation for more than 30 years. Pollack and co-workers believed that the observed spectroscopic changes are caused by anionization of the enolic or phenolic hydroxyl groups of the inhibitors upon binding to the active site.[41−44] One important piece of experimental evidence was that the UV−vis spectra of the KSI-bound phenol or naphthol inhibitors resemble the deprotonated, free phenolates in aqueous solution. In the meantime, Talalay and Mildvan et al. showed that the spectral changes are caused by polarization of the phenolic hydroxyl groups of the phenol or naphthol inhibitors by strong hydrogen bonding in the low-polarity environment of the enzyme active site.[40,45−48] Eventually, structural studies have revealed that ionization or polarization of the inhibitors is effected by two strong hydrogen bonds between the phenolic hydroxyl group of the inhibitors and the polar side chains of two active site residues, one tyrosine and one aspartic acid, which form an oxyanion hole responsible for stabilization of the enolate intermediate in enzyme catalysis.[49−52] Since then, KSI has been used as a model to study the roles of active site hydrogen bonding in enzyme catalysis.[53−55] More recently, Hammes-Schiffer and co-workers showed that deprotonation or polarization of the phenol and naphthol inhibitors is also affected by the electronic inductive effects from distal residues, which are exerted through a hydrogen bonding network.[56]

To test whether the observed spectroscopic changes of *Ec*MenB-bound DHNA-CoA analogues are due to deprotonation of their phenolic hydroxyl groups, these coenzyme A thioesters were dissolved in solution with an increasing pH value. As shown in Figure 3A for 1-HNA-CoA, the long-wavelength electronic absorption of the compound is progressively red-shifted from 368 nm at low pH values to 392 nm at pH >10 with a concurrent increase in the extinction coefficient. The midpoint pH value for the spectroscopic change in the titration is ~8.5, which is consistent with the expected pK_a value for the only phenolic hydroxyl group of the thioester. More importantly, the fully deprotonated 1-HNA-CoA at high pH gave rise to a new absorption peak at 323 nm, which is almost identical to the 325 nm new peak of the enzyme-bound 1-HNA-CoA in both peak position and intensity. Indeed, these deprotonation-induced spectral changes closely resemble that caused by the enzyme complexation, strongly suggesting that C1-OH in 1-HNA-CoA is similar to the phenolic hydroxyl groups of the KSI-bound inhibitors in being highly polarized or completely deprotonated by hydrogen bonding at the *Ec*MenB active site. Nonetheless, it should be noted that the enzyme-bound 1-HNA-CoA has a further 18 nm red shift and an irregular shape for the long-wavelength absorption in comparison to the free, fully deprotonated ligand (Figure 3A). This may be due to the difference in stabilization of the thioester phenolate in the two different solvent environments. The phenolate-stabilizing

hydrogen bonds are stronger in the low-polarity environment at the enzyme active site in comparison to the highly polar aqueous solution, leading to more pronounced changes in its electronic properties. Similar solvent effects have been demonstrated for the KSI-binding phenol or naphthol inhibitors.[40,46]

Deprotonation by pH titration and *Ec*MenB binding were also found to cause closely resembling spectroscopic changes in salicylyl-CoA and 2,4-DHB-CoA. As shown in Figure 3B, a progressive 42 nm red shift was found for salicylyl-CoA without the formation of any new absorption peaks when it was fully deprotonated in the pH titration (measured pK_a of ≈9.5), similar to the 62 nm red shift caused by complexation with *Ec*MenB. Similar comparison of the deprotonation effect and enzyme complexation was not successful for 2,3-DHB-CoA and DHNA-CoA because these thioesters decomposed at pH >8.5. Despite the lack of direct experimental support, both of the latter thioesters are believed to undergo deprotonation at C1-OH (DHNA-CoA) or its equivalent by hydrogen bonding interactions at the *Ec*MenB active site in consideration of their similar spectral changes, inhibition properties, and binding stoichiometry in comparison to those of other DHNA-CoA analogues.

Site-Directed Mutation of the Polar Active Site Residues in *Ec*MenB. Except for the bicarbonate cofactor that was known not to affect the spectral changes of DHNA-CoA and its analogues, other conserved polar residues at the *Ec*MenB active site were individually mutated to identify the functional groups involved in hydrogen bonding interactions with the hydroxyl groups of DHNA-CoA. Tyr-258 and Ser-161, whose equivalents in *Mtb*MenB were thought to form hydrogen bonds with C4-OH in DHNA-CoA in the late steps of catalysis,[7] were mutated to phenylalanine (Y258F) and alanine (S161A), respectively. In addition, the conserved Asp-163 was mutated to alanine (D163A), glutamate (D163E), and asparagine (D163N). Moreover, Arg-91 and Tyr-97, two strictly conserved polar residues on a disordered active site loop whose ordering was proposed to protect reactive reaction intermediates from the bulk solvent,[7] were mutated to alanine (R91A) and phenylalanine (Y97F), respectively. Moreover, Tyr-94, a nonconservative residue in the disordered active site loop, was mutated to phenylalanine (Y94F) as a negative control.

Except for S161A, which was expressed in inclusion bodies and unavailable for the binding test, all other mutants were readily obtained in high purity and found not to exhibit significant conformational changes by exhibiting a circular dichroism spectrum essentially identical to that of the wild-type protein. No DHNA-CoA synthetic activity was detected for mutants R91A, Y97F, D153, D163N, and Y258F, while D163E was found to possess 14% of the activity of the wild-type enzyme at a saturating concentration of the substrate. In contrast, Y94F exhibits the same level of activity as the wild-type *Ec*MenB, demonstrating that it is not involved in the recognition of the substrate or stabilization of reaction intermediates. This is supported by the finding that Y94F binds DHNA-CoA with exactly the same spectral changes as the wild-type protein (Figure 4A).

Tyr-258 Is Hydrogen-Bonded to C4-OH of DHNA-CoA. Using spectroscopic measurement, Y258F was found to bind DHNA-CoA and cause a red shift of the small molecule ligand from 392 to 432 nm (Figure 4A), similar to the spectral changes observed for the binding of 1-HNA-CoA or hydroxylated benzoyl-CoA to *Ec*MenB, although it is not clear whether there is an additional peak around 348 nm due to the strong absorption in the shifted spectrum. This similarity indicates that the interaction at C4-OH of DHNA-CoA is weakened or eliminated by

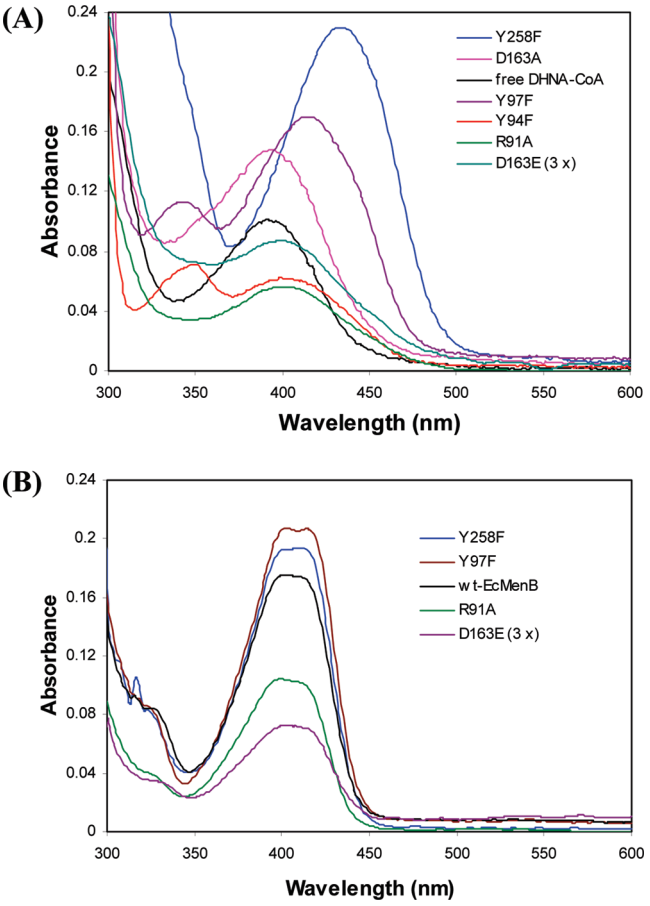

Figure 4. UV−vis spectra of DHNA-CoA (A) or 1-HNA-CoA (B) in complex with *Ec*MenB and its mutants. All enzyme−ligand interactions occurred in 200 mM sodium phosphate buffer (pH 7.0) containing 10 mM $NaHCO_3$. (A) Y258F: 30 μM Y258F and 15 μM DHNA-CoA. Y97F: 30 μM Y97F and 15 μM DHNA-CoA. Y94F: 29.7 μM Y94F and 6.6 μM DHNA-CoA. R91A: 75.9 μM R91A and 6.45 μM DHNA-CoA. D163E (3×): 180 μM D163E and 3.5 μM DHNA-CoA (spectrum magnified 3 times). (B) Y258F: 150 μM Y258F and 20.4 μM 1-HNA-CoA. Y97F: 64 μM Y97F and 20.4 μM 1-HNA-CoA. wt-*Ec*MenB: 62.8 μM wild-type *Ec*MenB and 20.4 μM 1-HNA-CoA. R91A: 75.9 μM R91A and 10.5 μM 1-HNA-CoA. D163E (3×): 235 μM D163E and 3.4 μM 1-HNA-CoA (spectrum magnified 3 times).

the Y258F mutation, providing direct experimental support for the proposed hydrogen bonding interaction between the side chain hydroxyl of Tyr-258 and C4-OH of DHNA-CoA in enzyme catalysis.[7] In addition, the observed similarity is also consistent with our proposal that the spectral changes for DHNA-CoA in complex with *Ec*MenB result from the additive effects of hydrogen bonding interactions at both C1- and C4-OH of the small molecule ligand: when interactions at C4-OH are weakened or eliminated in Y258F, the hydrogen bonding interactions at C1-OH cause a red shift of the DHNA-CoA absorption similar to that observed for the enzyme-bound analogues with only one hydroxyl group corresponding to C1-OH of DHNA-CoA, such as 1-HNA-CoA and salicylyl-CoA.

Tyr-97 and Arg-91 Interact Indirectly with C4-OH of DHNA-CoA. In contrast to the lack of any functional effects for the mutation at a nonconserved residue (Tyr-94) in the disordered active site loop of *Ec*MenB and *St*MenB (Figure 1B), mutation at the two strictly conserved polar residues in the same loop, Arg-91

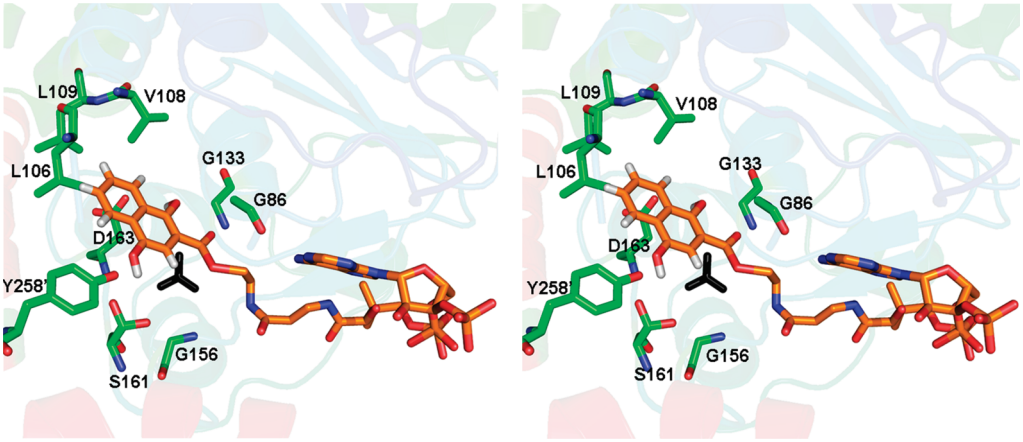

Figure 5. Stereoview of a model of the DHNA-CoA product in the active site of *St*MenB. The conserved active site residues are represented as sticks with green carbon atoms, and the modeled DHNA-CoA is represented as sticks with rainbow-colored atoms. The carbon atom of the bicarbonate cofactor is labeled in black. The primed residue (Y258′) is from a different subunit of the protein. The two-step modeling is described in the text using the *St*MenB (PDB entry 3H02) and *Mtb*MenB (PDB entry 1Q51) structures.

and Tyr-97, not only greatly diminishes the enzyme's catalytic activity but also significantly affects DHNA-CoA binding. Both R91A and Y97F mutants were found to bind DHNA-CoA with spectral changes. In the Y97F mutant, the 392 nm absorption of DHNA-CoA is red-shifted to 413 nm while a new, moderately intense peak is formed at 340 nm for the mutant−DHNA-CoA complexes (Figure 4A). These spectral changes are similar to those found for DHNA-CoA or 1-HNA-CoA in their interaction with wild-type *Ec*MenB, suggesting that the dominant hydrogen bonding at C1-OH of the bound DHNA-CoA is not disrupted by the Y97F mutation. Indeed, this was confirmed by the identical ultraviolet spectra for 1-HNA-CoA in complex with wild-type *Ec*MenB or the mutants (Figure 4B). In contrast, complexation by R91A causes an only 8 nm red shift of the DHNA-CoA absorption maxima to 400 nm without detectable absorption at 348 nm, which seems to suggest that Arg-91 interacts with C1-OH of the small molecule ligand. However, 1-HNA-CoA bound by R91A has exactly the same UV−vis spectrum as when it is bound by wild-type *Ec*MenB or other mutants (Figure 4B), indicating that Arg-91 does not directly interact with C1-OH of the small molecule ligand.

One explanation for the observed spectroscopic effects of the Y97F mutation is a direct hydrogen bonding interaction between the Tyr-97 polar side chain and C4-OH of the bound DHNA-CoA. Another way for Tyr-97 to affect the enzyme−ligand interaction is to form a hydrogen bond to the hydroxyl group of either Tyr-258 or Ser-161 to form a hydrogen bonding network and affect the electronic properties of the bound ligand through electronic inductive effects, similar to the effects of distal hydrogen bonds on the electronic properties of the bound ligands in KSI.[56] On the other hand, the role of Arg-91 is more complicated in the interaction with the small molecule ligands. Without conflicting with the possibility that Arg-91 may interact with Tyr-258 or Ser-161 through hydrogen bonding, mutation of the positive side chain may cause rearrangement of local active site residues that may result in unfavorable interaction with C4-OH. This suspected unfavorable interaction at C4-OH may in turn affect the binding interaction at C1-OH of DHNA-CoA, resulting in the small spectral changes for the R91A−ligand complex. In the absence of this unfavorable interaction, 1-HNA-CoA binds the R91A mutant in exactly the same way it binds the wild-type protein or the Y258F and Y97F mutants. Importantly, the spectral alterations observed for both R91A and Y97F mutants clearly indicate that the disordered loop at the enzyme active site (Figure 1B) is ordered upon binding of DHNA-CoA or its analogues for both residues to interact with the bound small molecule ligands.

Asp-163 Interacts with C1-OH of DHNA-CoA. Using optical spectrometry, D163A was not found to bind DHNA-CoA. No spectral changes were found for DHNA-CoA or 1-HNA-CoA in the presence of high concentrations of D163A (Figure 4A). However, both D163E and D163N were found to bind the small molecule ligands and to cause changes in their UV−vis spectra in a manner similar to that of the wild-type enzyme. The 392 nm absorption of DHNA-CoA was red-shifted to 400 nm with apparent absorption at ∼350 nm upon formation of the complex with D163E (Figure 4A), while the D163E-bound 1-HNA-CoA presented an electronic absorption spectrum identical to that of the *Ec*MenB-bound ligand (Figure 4B). D163N was found to be almost identical to D163E in causing spectral changes in the bound DHNA-CoA (Figure S5A of the Supporting Information) or 1-HNA-CoA (Figure S5B of the Supporting Information). These results provide unambiguous evidence that the carboxyl side chain of Asp-163 strongly interacts with C1-OH of the small molecule ligands as a major contributor to binding affinity.

Modeling of the Enzyme−Ligand Complex and Interaction at C1-OH of DHNA-CoA. To have a clearer picture of how DHNA-CoA interacts with the enzyme, the small molecule is modeled into the active site of *St*MenB, which is essentially identical to *Ec*MenB (96.8% identical sequences). The apo-*St*MenB structure was first superimposed on the structure of *Mtb*MenB in complex with the acetoacetyl-CoA to obtain a complex of *St*MenB with acetoacetyl-CoA, assuming that the thioester binds to the two proteins in the same way. Next, the acetoacetyl group was removed from the model structure and substituted with the 1,4-dihydroxy-2-naphthoyl group without changing the orientation of the thioester function. Subsequently, the naphthoyl group was slightly rotated against the C−S bond so that the carbonyl oxygen was within hydrogen bonding distance of both Gly-86 and Gly-133 that form the enolate-stabilizing oxyanion hole, while C4-OH was closest to the hydroxyl groups in the side chains of Tyr-258 and Ser-OH. The final model structure is shown in Figure 5 in which the phenolic oxygen of Tyr-258 and O^{γ} of Ser-161 are

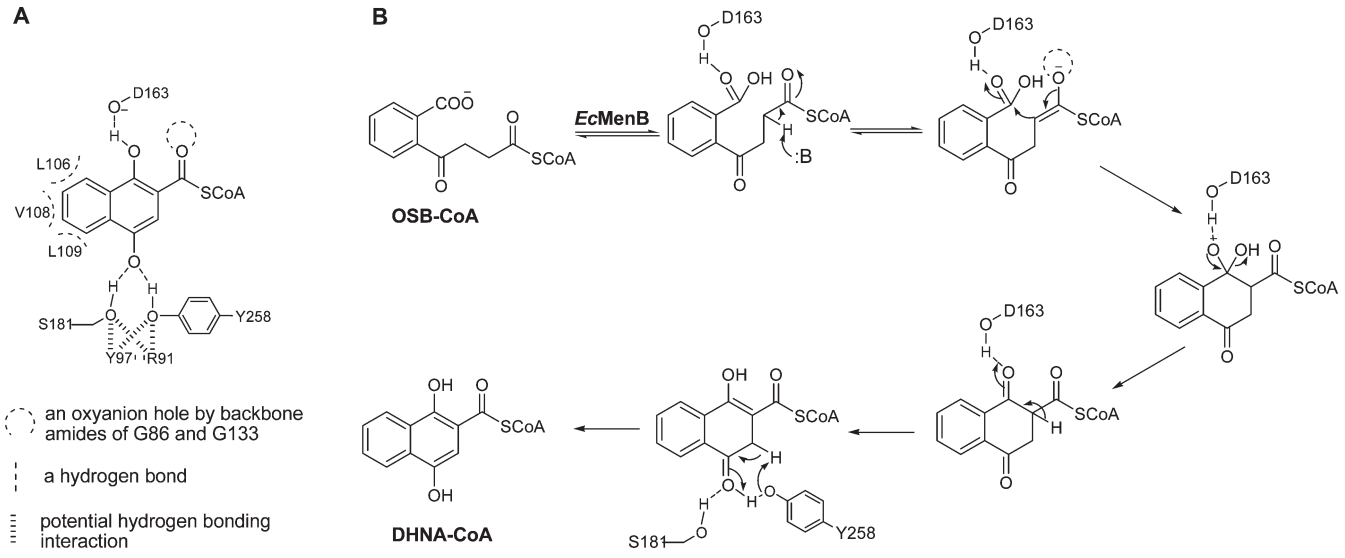

Figure 6. (A) Interaction of DHNA-CoA with the MenB active site. (B) Proposed roles of Asp-163 in the catalytic mechanism for the MenB-catalyzed reaction. The active site residues are numbered as they are in *Ec*MenB and are shown only at selected steps.

within hydrogen bonding distance (<4 Å) of the oxygen of C4-OH in the modeled DHNA-CoA. This model structure is consistent with the spectroscopic results for the Y258F mutant and the proposal that Tyr-258 and Ser-161 form hydrogen bonds with C4-OH of DHNA-CoA.

In the model structure, no backbone amide is close enough to C1-OH of DHNA-CoA to form a hydrogen bond. The closest polar groups to this hydroxyl group are the bicarbonate cofactor, which has been known not to affect the spectrum of the bound DHNA-CoA, and the γ-carboxyl group of Asp-163. The shorter distance between the oxygen atoms of the γ-carboxyl and the oxygen of the DHNA-CoA C1-OH group is 5.5 Å, which is greater than a hydrogen bonding distance. However, the Asp-163 side chain is flexible and is able to swing into a position to shorten the distance to <3.5 Å, making possible its hydrogen bond to C1-OH of DHNA-CoA. Therefore, this modeling result is consistent with the mutational results that support a strong hydrogen bond between the γ-carboxyl group of Asp-163 and C1-OH of the bound DHNA-CoA. Taking this into consideration, we summarize all possible interactions between the bound DHNA-CoA and *Ec*MenB in Figure 6A.

From the difference in affinity between salicylyl-CoA [K_D = 0.45 μM (Table 1)] and 3-HB-CoA (K_D > 10 mM), the apparent strength of the interaction at C1-OH of DHNA-CoA with the enzyme is calculated to be 4.0 kcal/mol, consistent with the strength of a normal hydrogen bond. The proposed hydrogen bonding of the Asp-163 side chain to the small molecule ligands seems to be enough to provide the needed binding energy. However, the actual strength of this interaction could be significantly greater than the apparent value because the binding energy may be used to overcome unfavorable interactions of other parts of the small molecule ligand with the enzyme active site. As such, the possibility that an additional hydrogen bond is formed between C1-OH of the bound DHNA-CoA and a yet unidentified active site function, which would together with the Asp-163 side chain form an oxyanion-like structure as found in KSI or other enzymes catalyzing reactions involving an oxyanion intermediate, could not be excluded. If existent, this unidentified function is likely a backbone amide either from the ordered active site residues or from the disordered active site loop (Figure 1B) because all the available conserved polar side chains except that of Asp-163 at the active site have been shown not to interact with C1-OH of the bound DHNA-CoA. In relation to this possibility, it is noted that nitrogen atoms of the backbone amides of the highly conserved Gly-132 and Gly-134 are within 6 Å of the oxygen of the C1-OH group of DHNA-CoA in the model complex.

Catalytic Mechanism of the MenB-Catalyzed Reaction. In the proposed reaction mechanism of the MenB-catalyzed intramolecular Claisen condensation reaction (Figure 1A), C1-OH of the DHNA-CoA product occupies a position similar to those of the carbonyl oxygen of the carboxyl group in the OSB-CoA substrate, the oxyanion in the tetrahedral oxyanion intermediate after the ring cyclization, and the oxygen species in other reaction intermediates. The likely hydrogen bonding between the *Ec*MenB Asp-163 side chain and C1-OH of the bound DHNA-CoA suggests that this polar group is also able to form a hydrogen bond to and stabilize the highly reactive tetrahedral oxyanion intermediate in the reaction process. We therefore propose that the Asp-163 side chain is responsible for stabilization of the high-energy tetrahedral oxyanion intermediate in the reaction mechanism. For the γ-carboxyl group of Asp-163 to stabilize an anion intermediate, its pK_a must be greatly increased by the active site environment to be protonated under physiological conditions. This is entirely possible in light of the fact that the pK_a of an oxyanion-stabilizing aspartate side chain is increased to >9.5 in KSI from a normal value of ~4.2.[57] However, pH titration of the enzyme−DHNA-CoA complex failed to produce direct supporting evidence of this pK_a change because of the complicated pH dependence of the interaction as shown in the parabolic relationship between A_{348} and pH (Figure S6 of the Supporting Information).

Considering the Asp-163 stabilization of the tetrahedral oxyanion intermediate and the expected ordering of the active site loop, we propose an induced-fit catalytic mechanism for the multistep synthesis of the naphthoyl product by *E. coli* DHNA-CoA synthase as shown in Figure 6B. In the catalysis, the binding of the OSB-CoA substrate to the MenB active site would induce folding of the disordered loop containing the conserved Arg-91 and Tyr-97

into an ordered structure so that the active site is sealed off from the bulk solvent to protect the reactive reaction intermediates as envisioned previously.[7] As a result of this induced fit, Arg-91, Tyr-97, Ser-161, and Tyr-258 may form a hydrogen bonding network to interact with the keto oxygen of the substrate and C4-OH of the DHNA-CoA product in later stage of the reaction, while the γ-carboxyl group of Asp-163 is hydrogen-bonded to the carbonyl oxygen of OSB-CoA. After abstraction of the α-proton by the bicarbonate cofactor with the stabilization of the oxyanion hole consisting of the backbone amides of two conserved glycine residues (Gly-86 and Gly-133), the hydrogen bonding interaction of the Asp-163 side chain facilitates the intramolecular condensation by stabilizing the tetrahedral oxyanion intermediate. The Asp-163 side chain would also polarize the carbonyl group formed after the Claisen condensation to facilitate its enolization to eventually form DHNA-CoA. At present, it is not clear how the tightly bound product is released from the active site after the synthesis. While further investigation is needed to solve this puzzle, it is tempting to speculate that the substrate-induced structural change in one subunit of the hexameric synthase might be able to cause a structural change in the neighboring subunit to discharge the bound product. The observed half-site occupancy of the *Ec*MenB active sites by DHNA-CoA is consistent with this hypothesis.

CONCLUSIONS

DHNA-CoA synthase is an essential enzyme in microbial menaquinone biosynthesis and a promising target for development of new antibiotics, for which no inhibitors have been reported. The identification of DHNA-CoA and its analogues as competitive inhibitors of the synthase in this study opens a venue to the development of new potent inhibitors and exploration of the synthase as a therapeutic target. In the meantime, the discovered exquisite sensitivity of the electronic structure of the inhibitors to their environment has allowed exploration of the enzyme−ligand interaction to provide important insights into the catalytic mechanism. On one hand, the similar effects of enzyme complexation and simple deprotonation on electronic absorptions indicate that the phenolic hydroxyl groups of the enzyme-bound ligands are highly polarized or anionized by hydrogen bonding interactions, while analysis of the structure−affinity relationships allows identification of C1-OH of DHNA-CoA or its equivalent as the dominant site for the polarizing interactions. On the other hand, mutagenic studies have provided evidence of the interaction of Arg-91, Tyr-97, and Tyr-258 with C4-OH of the enzyme-bound DHNA-CoA through a hydrogen bond network that also includes Ser-161, while the similar mutational results suggest that the side chain of Asp-163 is at least partly responsible for the polarizing effects on C1-OH of DHNA-CoA. All these experimental results point to the probability that the Asp-163 side chain is likely involved in stabilization of the high-energy tetrahedral oxyanion intermediate in the catalytic process. Because of the special location of Arg-91 and Tyr-97 in a flexible active site loop, the involvement of these two residues in the interaction with DHNA-CoA is a strong indication that the active site structure undergoes substantial change during enzyme catalysis. This structural change strongly suggests an induced-fit mechanism for the intramolecular Claisen condensation catalyzed by DHNA-CoA synthases. These findings have laid the groundwork for further exploration of the catalytic mechanism aimed at improving our understanding of DHNA-CoA synthase as a unique member of the crotonase fold protein superfamily.

ASSOCIATED CONTENT

Supporting Information. Supplementary figures, sodium dodecyl sulfate−polyacrylamide gel electrophoresis gel and circular dichroism spectra for the *E. coli* DHNA-CoA synthase and its mutants. This material is available free of charge via the Internet at http://pubs.acs.org.

AUTHOR INFORMATION

Corresponding Author

*Department of Chemistry, The Hong Kong University of Science and Technology, Clear Water Bay, Kowloon, Hong Kong SAR, China. Telephone: 852-2358-7352. Fax: 852-2358-1594. E-mail: chguo@ust.hk.

Present Addresses

[†]Department of Chemical and Biological Engineering, Tufts University, Medford, MA 02155.

[‡]Department of Pharmacology and Molecular Sciences, School of Medicine, Johns Hopkins University, Baltimore, MD 21211.

Funding Sources

This work was financially supported by Grant GRF601209 from the Research Grants Council of the Hong Kong Special Administrative Region of the People's Republic of China.

ACKNOWLEDGMENT

We thank Mr. Gary Wan and Professor Yundong Wu for help with protein graphics.

ABBREVIATIONS

CoA, coenzyme A; OSB-CoA, *o*-succinylbenzoyl-CoA; DHNA-CoA, 1, 4-dihydroxy-2-naphthoyl-CoA; SHCHC, (1*R*,6*R*)-2-succinyl-6-hydroxy-2,4-cyclohexadiene-1-carboxylate; HB, hydroxybenzoate or hydroxybenzoyl; DHB, dihydroxybenzoate or dihydroxybenzoyl; IPTG, isopropyl β-D-thiogalactopyranoside; DDT, dithiothreitol; *Ec*MenB, *Mtb*MenB, *St*MenB, *Sa*MenB, and *Ms*MenB, MenB orthologues from *E. coli*, *M. tuberculosis*, *Sa. typhimurium*, *S. aureus*, and *M. smegmatis*, respectively; KSI, Δ^5-3-ketosteroid isomerase; PDB, Protein Data Bank.

REFERENCES

(1) Meganathan, R. (2001) Biosynthesis of menaquinone (vitamin K2) and ubiquinone (coenzyme Q): A perspective on enzymatic mechanisms. *Vitam. Horm. 61*, 173–218.

(2) Forsyth, R. A., Haselbeck, R. J., Ohlsen, K. L., Yamamoto, R. T., Xu, H., Trawick, J. D., Wall, D., Wang, L., Brown-Driver, V., Froelich, J. M., Kedar, G. C., King, P., McCarthy, M., Malone, C., Misiner, B., Robbins, D., Tan, Z., Zhu, Z.-y., Carr, G., Mosca, D. A., Zamudio, C., Foulkes, J. G., and Zyskind, J. W. (2002) A genome-wide strategy for the identification of essential genes in *Staphylococcus aureus*. *Mol. Microbiol. 43*, 1387–1400.

(3) Kobayashi, K., Ehrlich, S. D., Albertini, A., Amati, G., Andersen, K. K., Arnaud, M., Asai, K., Ashikaga, S., Aymerich, S., Bessieres, P., Boland, F., Brignell, S. C., Bron, S., Bunai, K., Chapuis, J., Christiansen, L. C., Danchin, A., Débarbouille, M., Dervyn, E., Deuerling, E., Devine, K., Devine, S. K., Dreesen, O., Errington, J., Fillinger, S., Foster, S. J., Fujita, Y., Galizzi, A., Gardan, R., Eschevins, C., Fukushima, T., Haga, K.,

Harwood, C. R., Hecker, M., Hosoya, D., Hullo, M. F., Kakeshita, H., Karamata, D., Kasahara, Y., Kawamura, F., Koga, K., Koski, P., Kuwana, R., Imamura, D., Ishimaru, M., Ishikawa, S., Ishio, I., Le Coq, D., Masson, A., Mauël, C., Meima, R., Mellado, R. P., Moir, A., Moriya, S., Nagakawa, E., Nanamiya, H., Nakai, S., Nygaard, P., Ogura, M., Ohanan, T., O'Reilly, M., O'Rourke, M., Pragai, Z., Pooley, H. M., Rapoport, G., Rawlins, J. P., Rivas, L. A., Rivolta, C., Sadaie, A., Sadaie, Y., Sarvas, M., Sato, T., Saxild, H. H., Scanlan, E., Schumann, W., Seegers, J. F., Sekiguchi, J., Sekowska, A., Séror, S. J., Simon, M., Stragier, P., Studer, R., Takamatsu, H., Tanaka, T., Takeuchi, M., Thomaides, H. B., Vagner, V., van Dijl, J. M., Watabe, K., Wipat, A., Yamamoto, H., Yamamoto, M., Yamamoto, Y., Yamane, K., Yata, K., Yoshida, K., Yoshikawa, H., Zuber, U., and Ogasawara, N. (2003) Essential *Bacillus subtilis* genes. *Proc. Natl. Acad. Sci. U.S.A. 100*, 4678–4683.

(4) Akerley, B. J., Rubin, E. J., Novick, V. L., Amaya, K., Judson, N., and Mekalanos, J. J. (2002) A genome-scale analysis for identification of genes required for growth or survival of *Haemophilus influenzae*. *Proc. Natl. Acad. Sci. U.S.A. 99*, 966–971.

(5) Kurosu, M., Narayanasamy, P., Biswas, K., Dhiman, R., and Crick, D. C. (2007) Discovery of 1,4-dihydroxy-2-naphthoate prenyltransferase inhibitors: New drug leads for multidrug-resistant Gram-positive pathogens. *J. Med. Chem. 50*, 3973–3975.

(6) Dhiman, R. K., Mahapatra, S., Slayden, R. A., Boyne, M. E., Lenaerts, A., Hinshaw, J. C., Angala, S. K., Chatterjee, D., Biswas, K., Narayanasamy, P., Kurosu, M., and Crick, D. C. (2009) Menaquinone synthesis is critical for maintaining mycobacterial viability during exponential growth and recovery from non-replicating persistence. *Mol. Microbiol. 72*, 85–97.

(7) Truglio, J. J., Theis, K., Feng, Y., Gajda, R., Machutta, C., Tonge, P. J., and Kisker, C. (2003) Crystal structure of *Mycobacterium tuberculosis* MenB, a key enzyme in vitamin K_2 biosynthesis. *J. Biol. Chem. 278*, 42352–42360.

(8) Hamed, R. B., Batchelar, E. T., Clifton, I. J., and Schofield, C. J. (2008) Mechanisms and structures of crotonase superfamily enzymes: How nature controls enolate and oxyanion reactivity. *Cell. Mol. Life Sci. 65*, 2507–2527.

(9) Holden, H. M., Benning, M. M., Haller, T., and Gerlt, J. A. (2001) The crotonase superfamily: Divergently related enzymes that catalyze different reactions involving acyl coenzyme A thioesters. *Acc. Chem. Res. 34*, 145–157.

(10) Johnston, J. M., Arcus, V. L., and Baker, E. N. (2005) Structure of naphthoate synthase (MenB) from *Mycobacterium tuberculosis* in both native and product-bound forms. *Acta Crystallogr. D61*, 1199–1206.

(11) Ulaganathan, V., Agacan, M. F., Buetow, L., Tulloch, L. B., and Hunter, W. N. (2007) Structure of *Staphylococcus aureus* 1,4-dihydroxy-2-naphthoyl-CoA synthase (MenB) in complex with acetoacetyl-CoA. *Acta Crystallogr. F63*, 908–913.

(12) D'Ordine, R. L., Bahnson, B. J., Tonge, P. J., and Anderson, V. E. (1994) Enoyl-coenzyme A hydratase-catalyzed exchange of the α-protons of coenzyme A thiol esters: A model for an enolized intermediate in the enzyme-catalyzed elimination? *Biochemistry 33*, 14733–14742.

(13) Müller-Newen, G., Janssen, U., and Stoffel, W. (1995) Enoyl-CoA hydratase and isomerase form a superfamily with a common active-site glutamate residue. *Eur. J. Biochem. 228*, 68–73.

(14) Engel, C. K., Mathieu, M., Zeelen, J. P., Hiltunen, J. K., and Wierenga, R. K. (1996) Crystal structure of enoyl-coenzyme A (CoA) hydratase at 2.5 Å resolution: A spiral fold defines the CoA-binding pocket. *EMBO J. 15*, 5135–5145.

(15) Engel, C. K., Kiema, T. R., Hiltunen, J. K., and Wierenga, R. K. (1998) The crystal structure of enoyl-CoA hydratase complexed with octanoyl-CoA reveals the structural adaptations required for binding of a long chain fatty acid-CoA molecule. *J. Mol. Biol. 275*, 847–859.

(16) Modis, Y., Filppula, S. A., Novikov, D. K., Norledge, B., Hiltunen, J. K., and Wierenga, R. K. (1998) The crystal structure of dienoyl-CoA isomerase at 1.5 Å resolution reveals the importance of aspartate and glutamate side chains for catalysis. *Structure 6*, 957–970.

(17) Kiema, T.-R., Engel, C. K., Schmitz, W., Filppula, S. A., Wierenga, R. K., and Hiltunen, J. K. (1999) Mutagenic and enzymological studies of the hydratase and isomerase activities of 2-enoyl-CoA hydratase-1. *Biochemistry 38*, 2991–2999.

(18) Mursula, A. M., van Aalten, D. M., Hiltunen, J. K., and Wierenga, R. K. (2001) The crystal structure of Δ^3-Δ^2-enoyl-CoA isomerase. *J. Mol. Biol. 309*, 845–853.

(19) Jiang, M., Chen, M., Guo, Z.-F., and Guo, Z. (2010) A bicarbonate cofactor modulates 1,4-dihydroxy-2-naphthoyl coenzyme A synthase in menaquinone biosynthesis of *Escherichia coli*. *J. Biol. Chem. 285*, 30159–30169.

(20) Kraut, J. (1977) Serine proteases: Structure and mechanism of catalysis. *Annu. Rev. Biochem. 46*, 331–358.

(21) Holmquist, M. (2000) α/β-Hydrolase fold enzymes: Structures, functions and mechanisms. *Curr. Protein Pept. Sci. 1*, 209–235.

(22) Smith, S., Witkowski, A., and Joshi, A. K. (2003) Structural and functional organization of the animal fatty acid synthase. *Prog. Lipid Res. 42*, 289–317.

(23) White, S. W., Zheng, J., Zhang, Y.-M., and Rock, C. O. (2005) The structural biology of type II fatty acid biosynthesis. *Annu. Rev. Biochem. 74*, 791–831.

(24) Machutta, C. A., Bommineni, G. R., Luckner, S. R., Kapilashrami, K., Ruzsicska, B., Simmerling, C., Kisker, C., and Tonge, P. J. (2010) Slow onset inhibition of bacterial β-ketoacyl-acyl carrier protein synthases by thiolactomycin. *J. Biol. Chem. 285*, 6161–6169.

(25) Witkowski, A., Joshi, A. K., Lindqvist, Y., and Smith, S. (1999) Conversion of a β-ketoacyl synthase to a malonyl decarboxylase by replacement of the active-site cysteine with glutamine. *Biochemistry 38*, 11643–11650.

(26) Jiang, M., and Guo, Z. (2007) Effects of macromolecular crowding on the intrinsic catalytic efficiency and structure of enterobactin-specific isochorismate synthase. *J. Am. Chem. Soc. 129*, 730–731.

(27) Guo, Z.-F., Jiang, M., Zheng, S., and Guo, Z. (2008) Suppression of linear side products by macromolecular crowding in nonribosomal enterobactin biosynthesis. *Org. Lett. 10*, 649–652.

(28) Jiang, M., Cao, Y., Guo, Z.-F., Chen, M., Chen, X., and Guo, Z. (2007) Menaquinone biosynthesis in *Escherichia coli*: Identification of 2-succinyl-5-enolpyruvyl-6-hydroxy-3-cyclohexene-1-carboxylate (SEPHCHC) as a novel intermediate and re-evaluation of MenD activity. *Biochemistry 46*, 10979–10989.

(29) Jiang, M., Chen, M., Cao, Y., Yang, Y., Sze, K. H., Chen, X., and Guo, Z. (2007) Determination of the stereochemistry of 2-succinyl-5-enolpyruvyl-6-hydroxy-3-cyclohexene-1-carboxylic acid, a key intermediate in menaquinone biosynthesis. *Org. Lett. 9*, 4765–4767.

(30) Jiang, M., Chen, X., Guo, Z.-F., Cao, Y., Chen, M., and Guo, Z. (2008) Identification and characterization of (1*R*,6*R*)-2-succinyl-6-hydroxy-2,4-cyclohexadiene-1-carboxylate synthase in the menaquinone biosynthesis of *Escherichia coli*. *Biochemistry 47*, 3426–3434.

(31) Jiang, M., Chen, X., Wu, X.-H., Chen, M., Wu, Y., and Guo, Z. (2009) Catalytic mechanism of SHCHC synthase in the menaquinone biosynthesis of *Escherichia coli*: Identification and mutational analysis of the active site residues. *Biochemistry 48*, 6921–6931.

(32) Grisostomi, G., Kast, P., Pulido, R., Huynh, J., and Hilvert, D. (1997) Efficient in vivo synthesis and rapid purification of chorismic acid using an engineered *Escherichia coli* strain. *Bioorg. Chem. 25*, 297–305.

(33) Lai, M.-t., Li, D., Oh, E., and Liu, H.-w. (1993) Inactivation of medium-chain acyl-CoA dehydrogenase by a metabolite of hypoglycin: Characterization of the major turnover product and evidence suggesting an alternative flavin modification pathway. *J. Am. Chem. Soc. 115*, 1619–1628.

(34) Guo, Z.-F., Sun, Y., Zheng, S., and Guo, Z. (2009) Preferential hydrolysis of aberrant precursors suggests an active proofreading mechanism for the type II thioesterase in *Escherichia coli* enterobactin biosynthesis. *Biochemistry 48*, 1712–1722.

(35) DeLano, W. L. (2002) *The PyMOL Molecular Graphics System*, DeLano Scientific, San Carlos, CA.

(36) Emsley, P., and Cowtan, K. (2004) Coot: Model-building tools for molecular graphics. *Acta Crystallogr. D60*, 2126–2132.

(37) Gibson, R. E. (1976) Ligand interactions with the acetylcholine receptor from *Torpedo californica*. Extensions of the allosteric model for cooperativity to half-of-site activity. *Biochemistry 15*, 3890–3901.

(38) Brown, J. H. (2006) Breaking symmetry in protein dimers: Designs and functions. *Protein Sci. 15*, 1–13.

(39) Castellani, M., Covian, R., Kleinschroth, T., Anderka, O., Ludwig, B., and Trumpower, B. L. (2010) Direct demonstration of half-of-the-sites reactivity in the dimeric cytochrome bc_1 complex: Enzyme with one inactive monomer is fully active but unable to activate the second ubiquinol oxidation site in response to ligand binding at the ubiquinone reduction site. *J. Biol. Chem. 285*, 502–510.

(40) Wang, S.-F., Kawahara, F. S., and Talalay, P. (1963) The mechanism of the Δ^5-3-ketosteroid isomerase reaction: Absorption and fluorescence spectra of enzyme-steroid complexes. *J. Biol. Chem. 238*, 576–585.

(41) Eames, T. M., Pollack, R. M., and Steiner, R. F. (1989) Orientation, accessibility, and mobility of equilenin bound to the active site of steroid isomerase? *Biochemistry 28*, 6269–6275.

(42) Zeng, B., Bounds, P. L., Steiner, R. F., and Pollack, R. M. (1992) Nature of the intermediate in the 3-oxo-Δ^5-steroid isomerase yeaction? *Biochemistry 31*, 1521–1528.

(43) Petrounia, I. P., and Pollack, R. M. (1998) Substituent effects on the binding of phenols to the D38N mutant of 3-oxo-Δ^5-steroid isomerase. A probe for the nature of hydrogen bonding to the intermediate. *Biochemistry 37*, 700–705.

(44) Petrounia, I. P., Blotny, G., and Pollack, R. M. (2000) Binding of 2-naphthols to D38E mutants of 3-oxo-Δ^5-steroid isomerase: Variation of ligand ionization state with the nature of the electrophilic component. *Biochemistry 39*, 110–116.

(45) Kuliopulos, A., Mildvan, A. S., Shortle, D., and Talalay, P. (1989) Kinetic and ultraviolet spectroscopic studies of active-site mutants of Δ^5-3-ketosteroid isomerase. *Biochemistry 28*, 149–159.

(46) Zhao, Q., Mildvan, A. S., and Talalay, P. (1995) Enzymatic and nonenzymatic polarizations of α,β-unsaturated ketosteroids and phenolic steroids. Implications for the roles of hydrogen bonding in the catalytic mechanism of Δ^5-3-ketosteroid isomerase. *Biochemistry 34*, 426–434.

(47) Austin, J. C., Zhao, Q., Jordan, T., Talalay, P., Mildvan, A. S., and Spiro, T. G. (1995) Ultraviolet resonance Raman spectroscopy of Δ^5-3-ketosteroid isomerase revisited: Substrate polarization by active-site residues. *Biochemistry 34*, 4441–4447.

(48) Zhao, Q., Abeygunawardana, C., Talalay, P., and Mildvan, A. S. (1996) NMR evidence for the participation of a low-barrier hydrogen bond in the mechanism of Δ^5-3-ketosteroid isomerase. *Proc. Natl. Acad. Sci. U.S.A. 93*, 8220–8224.

(49) Wu, Z., Ebrahimian, S., Zawrotny, M. E., Thornburg, L. D., Perez-Alvarado, G. C., Brothers, P., Pollack, R. M., and Summers, M. F. (1997) Solution structure of 3-oxo-Δ^5-steroid isomerase. *Science 276*, 415–418.

(50) Cho, H.-S., Choi, G., Choi, K. Y., and Oh, B.-H. (1998) Crystal structure and enzyme mechanism of Δ^5-3-ketosteroid isomerase from *Pseudomonas testosterone*. *Biochemistry 37*, 8325–8330.

(51) Cho, H.-S., Ha, N.-C., Choi, G., Kim, H.-J., Lee, D., Ohi, K. S., Kimi, K. S., Lee, W., Choi, K. Y., and Oh, B.-H. (1999) Crystal structure of Δ^5-3-ketosteroid isomerase from *Pseudomonas testosteroni* in complex with equilenin settles the correct hydrogen bonding scheme for transition state stabilization. *J. Biol. Chem. 274*, 32863–32868.

(52) Choi, G., Ha, N.-C., Kim, S. W., Kim, D.-H., Park, S., Oh, B.-H., and Choi, K. Y. (2000) Asp-99 donates a hydrogen bond not to Tyr-14 but to the steroid directly in the catalytic mechanism of Δ^5-3-ketosteroid isomerase from *Pseudomonas putida* biotype B. *Biochemistry 39*, 903–909.

(53) Kraut, D. A., Sigala, P. A., Pybus, B., Liu, C. W., Ringe, D., Petsko, G. A., and Herschlag, D. (2006) Testing electrostatic complementarity in enzyme catalysis: Hydrogen bonding in the ketosteroid isomerase oxyanion hole. *PLoS Biol. 4*, 0501–0519.

(54) Childs, W., and Boxer, S. G. (2010) Proton affinity of the oxyanion hole in the active site of ketosteroid isomerase. *Biochemistry 49*, 2725–2731.

(55) Krauta, D. A., Sigalaa, P. A., Fennb, T. D., and Herschlag, D. (2010) Dissecting the paradoxical effects of hydrogen bond mutations in the ketosteroid isomerase oxyanion hole. *Proc. Natl. Acad. Sci. U.S.A. 107*, 1960–1965.

(56) Hanoian, P., Sigala, P. A., Herschlag, D., and Hammes-Schiffer, S. (2010) Hydrogen bonding in the active site of ketosteroid isomerase: Electronic inductive effects and hydrogen bond coupling. *Biochemistry 49*, 10339–10348.

(57) Thornburg, L. D., Hénot, F., Bash, D. P., Hawkinson, D. C., Bartel, S. D., and Pollack, R. M. (1998) Electrophilic assistance by Asp-99 of 3-oxo-Δ^5-steroid isomerase. *Biochemistry 37*, 10499–10506.